BIOCHEMISTRY
including biophysical chemistry & molecular biology
Article

Biochemistry **2010,** *49,* 5899–5908 5899
DOI: 10.1021/bi902197x

Inhibition by Flavonoids of Amyloid-like Fibril Formation by *Plasmodium falciparum* Merozoite Surface Protein 2[†]

Indu R. Chandrashekaran,[‡] Christopher G. Adda,[§] Christopher A. MacRaild,[‡] Robin F. Anders,[§] and Raymond S. Norton*[,‡]

[‡]*The Walter and Eliza Hall Institute of Medical Research, 1G Royal Parade, Parkville, Victoria 3052, Australia, and* [§]*Department of Biochemistry, La Trobe University, Victoria 3086, Australia*

Received December 23, 2009; Revised Manuscript Received May 17, 2010

ABSTRACT: Merozoite surface protein 2 (MSP2) is a glycosylphosphatidylinositol (GPI)-anchored protein expressed abundantly on the surface of *Plasmodium falciparum* merozoites. The results of a phase 2 trial in Papua New Guinean children showed MSP2 to be a promising malaria vaccine candidate. MSP2 is intrinsically unstructured and forms amyloid-like fibrils under physiological conditions. Oligomers containing β-strand interactions similar to those in amyloid fibrils may be a component of the fibrillar surface coat on *P. falciparum* merozoites. As the propensity of MSP2 to form fibrils in solution also has the potential to impede its development as a vaccine candidate, finding an inhibitor that specifically inhibits fibrillogenesis may enhance vaccine development. In this study, we tested the ability of three flavonoids, EGCG, baicalein, and resveratrol, to inhibit MSP2 fibrillogenesis and found marked inhibition with EGCG but not with the other two flavonoids. The inhibitory effect and the interactions of the flavonoids with MSP2 were characterized using NMR spectroscopy, thioflavin T fluorescence assays, electron microscopy, and other biophysical methods. EGCG stabilizes soluble oligomers and blocks fibrillogenesis by preventing the conformational transition of MSP2 from a random coil to an amyloidogenic β-sheet structure. Structural comparison of the three flavonoids indicates an association between their propensity for autoxidation and their fibril inhibitory activity; the activity of EGCG can be attributed to the vicinal hydroxyl groups present in this flavonoid and their ability to form quinones. The molecular mechanism of fibril inhibition by EGCG appears to be complex and involves noncovalent binding followed by covalent modification of the protein. Although the addition of EGCG appears to be an effective means of stabilizing MSP2 in solution, the covalent modification of MSP2 would most likely not be acceptable in a vaccine formulation. However, these small molecule inhibitors of MSP2 fibril formation will be useful as mechanistic probes in studying oligomerization and fibril assembly of MSP2.

Plasmodium falciparum, the causative agent of the most severe form of malaria, infects up to 500 million people and results in close to 1 million deaths annually (*1*, *2*). Malaria remains one of the most prevalent diseases in many developing countries, with young children living in malaria-endemic regions who have not developed protective adaptive immune responses to the parasite being most at risk (*3*). The development of a vaccine against *P. falciparum* remains one of the major priorities for addressing this global health problem. Merozoite surface proteins from the asexual blood stage of the parasite are considered important potential components of such a vaccine. Merozoite surface protein 2 (MSP2),[1] a glycosylphosphatidylinositol (GPI)-anchored protein expressed on the merozoite surface (*4*, *5*), is thought to have a role in erythrocyte invasion and hence is a potential vaccine candidate. Indeed, MSP2 was one of three components of a combination vaccine that significantly reduced parasite densities when tested in a phase 2 trial in Papua New Guinean children (*6*).

Mature MSP2 has conserved N- and C-terminal domains of 25 and ~50 residues, respectively, and a highly polymorphic central variable region (*7*, *8*). The central polymorphic region contains tandemly arrayed repetitive sequences flanked by nonrepetitive sequences, which define the two allelic families of MSP2, 3D7 and FC27 (*8*, *9*). Full-length MSP2 has the characteristics of an intrinsically unstructured protein and forms amyloid-like fibrils in solution under physiological conditions (*10*, *11*). These fibrils have a proteinase K-resistant core comprised of the conserved N-terminal region of MSP2 (*10*). Recent studies have shown that peptides from this region form fibrils similar to those formed by full-length MSP2 (*12*, *13*). It may be that the conserved N-terminal region of MSP2 nucleates the intermolecular interactions that result in the formation of amyloid-like fibrils (*10*, *12*, *13*). As the propensity of MSP2 to form fibrils in solution is potentially problematic for vaccine development, finding an inhibitor that specifically inhibits MSP2 fibril formation could assist the development of MSP2 as a vaccine candidate.

Various small molecules, including some polyphenols, have been reported to inhibit amyloid fibril formation by other proteins (*14*). Flavonoids, a group of plant-derived polyphenolic compounds

[†]This work was supported in part by National Institutes of Health Grant R01AI59229 (to R.F.A. and R.S.N.), as well as NHMRC IRIISS Grant 361646 and a Victorian State Government OIS grant. R.S.N. acknowledges fellowship support from the NHMRC.

*To whom correspondence should be addressed: The Walter and Eliza Hall Institute of Medical Research, 1G Royal Parade, Parkville, Victoria 3052, Australia. Phone: +61 3 9345 2306. Fax: +61 3 9345 2686. E-mail: ray.norton@wehi.edu.au.

[1]Abbreviations: BSA, bovine serum albumin; CD, circular dichroism; EGCG, (−)-epigallocatechin gallate; FC27 MSP2-6H, C-terminally His-tagged full-length FC27 MSP2; FC27 NT-MSP2, untagged full-length FC27 MSP2; GPI, glycosylphosphatidylinositol; HSQC, heteronuclear single-quantum coherence; mAbs, monoclonal antibodies; MSP2, merozoite surface protein 2; NBT, nitroblue tetrazolium; N-MSP2, N-terminal region of MSP2; PBS, phosphate-buffered saline; SEC, size-exclusion chromatography; TEM, transmission electron microscopy; ThT, thioflavin T.

Published on Web 06/14/2010

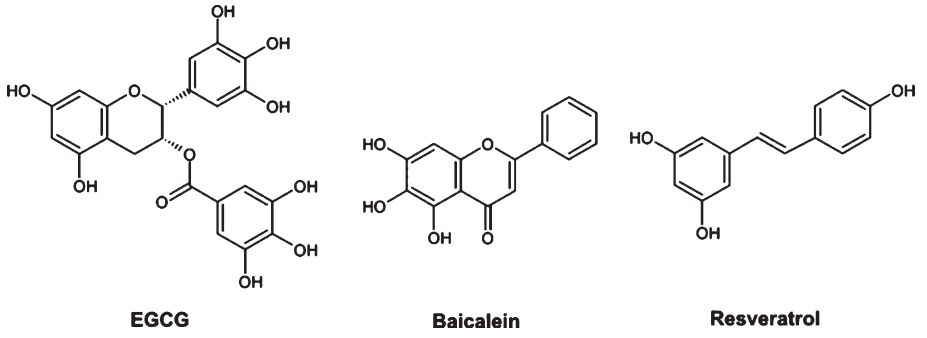

FIGURE 1: Chemical structures of (−)-epigallocatechin gallate (EGCG), baicalein, and resveratrol.

with broad pharmacological activities, are important components in the human diet and medicinal plants (*15*). In recent years, these compounds have attracted significant research interest because of their antioxidant, antitumor, and antimicrobial activities, in addition to their effects on amyloid fibril formation (*14*−*16*). Flavonoids have been shown to inhibit fibrillogenesis by amyloidogenic proteins in vitro, in cell culture, and, recently, in vivo (*17*−*19*). Their inhibition of fibril formation by more than one amyloidogenic protein suggests that flavonoids have a generic mode of action (*17*, *20*).

(−)-Epigallocatechin gallate (EGCG) (Figure 1), the most abundant flavonoid in green tea, has received attention for its ability to inhibit fibrillogenesis (*17*, *21*). EGCG efficiently inhibits amyloid fibril formation by several amyloidogenic proteins involved in neurodegenerative diseases, including α-synuclein, Aβ, and huntingtin (*17*, *21*, *22*). In a recent study, EGCG was shown to redirect aggregation-prone proteins like Aβ and α-synuclein into off-pathway oligomers and thus prevent fibril formation (*17*). Other flavonoids with similar activity are baicalein and resveratrol (Figure 1). Baicalein, the main component of a traditional Chinese herbal medicine, is neuroprotective and inhibits fibril formation by α-synuclein (*18*, *19*). Resveratrol, a major flavonoid constituent of grapes and red wine, has been shown to inhibit amyloid fibril formation by Aβ and IAPP (*23*−*25*) and to reduce secreted and intracellular Aβ levels (*23*).

In this study, we have investigated the inhibitory effects of EGCG, baicalein, and resveratrol on amyloid-like fibril formation by MSP2. NMR spectroscopy, thioflavin T assays, electron microscopy, and other biophysical methods have been used to explore the flavonoid−MSP2 interactions and their inhibitory effects on fibril formation. We show that EGCG is an efficient and potent inhibitor of MSP2 fibril formation and stabilizes soluble oligomers of MSP2.

MATERIALS AND METHODS

Materials. EGCG was obtained from Sigma, and stock solutions were freshly prepared in water. Stock solutions of baicalein and resveratrol, also obtained from Sigma, were freshly prepared in DMSO. As DMSO contributes strongly to the far-UV CD spectrum, baicalein and resveratrol stocks used for CD studies were prepared in methanol.

Protein Expression and Purification. All of the studies described here were conducted with the recombinant FC27 allelic form of MSP2 expressed in *Escherichia coli*. Two different constructs were used for the studies: C-terminally His_6-tagged full-length FC27 MSP2 (FC27 MSP2-6H) and untagged full-length FC27 MSP2 (FC27 NT-MSP2). FC27 MSP2-6H was purified by metal chelate chromatography, followed by anion-exchange and reverse-phase chromatography (*10*, *11*). FC27 NT-MSP2 was purified using a strategy specific for recombinantly expressed unstructured proteins, as described previously (*11*). Immediately prior to all experiments, MSP2 was heated to 90 °C for 5 min, cooled on ice for 2 min, and filtered through a 0.02 μm membrane to ensure that only monomeric MSP2 was present. The peptide corresponding to the conserved N-terminal region of MSP2 (N-MSP2) was synthesized as described previously (*13*).

Thioflavin T Fluorescence Assays. The time course of MSP2 aggregation was monitored using thioflavin T (ThT) (Sigma), a fluorophore that increases its fluorescence intensity upon binding to amyloid fibrils (*26*). To determine whether flavonoids inhibit MSP2 fibrillogenesis, we assessed aggregation of both FC27 MSP2-6H and FC27 NT-MSP2 using changes in ThT fluorescence in the presence of the flavonoids. An EGCG stock solution (16 mM) was prepared in water, and baicalein (40 mM) and resveratrol (20 mM) stock solutions were prepared in DMSO. Reactions in 200 μL volumes were conducted in black 96-well microtiter plates (Nunc) containing 40 μM FC27 MSP2-6H monomer and 30 μM ThT in PBS. Aliquots from flavonoid stocks were added to the wells to yield a final concentration of 400 μM for EGCG and 600 μM for baicalein and resveratrol. The final DMSO concentration in baicalein and resveratrol samples was 1.5% (v/v). Control MSP2 samples containing 1.5% (v/v) DMSO were also prepared. The microtiter plates were sealed with self-adhesive plate covers to reduce evaporation. ThT fluorescence was assayed at 10 min intervals following agitation (20 s) of the plate, using a SpectroMax M2 plate reader (Molecular Devices) at excitation and emission wavelengths of 443 and 484 nm, respectively. All data were normalized to the maximum ThT signal. Single-time point ThT assays were also set up to monitor the kinetics of MSP2 fibril formation in the presence of different concentrations of flavonoids (40, 200, 400, and 600 μM). The baicalein and resveratrol stocks used for this assay were prepared in methanol; the final methanol concentration in baicalein and resveratrol samples was 4% (v/v). FC27 MSP2-6H (40 μM) was incubated with and without flavonoids for 48 h in microfuge tubes on a rotator at room temperature. Control MSP2 samples containing 4% (v/v) methanol were also prepared. Aliquots were removed at various intervals and diluted (to 10 μM), and then ThT was added to a final concentration of 30 μM. ThT fluorescence was assayed in microtiter plates at each time point, using a SpectroMax M2 plate reader (Molecular Devices) at excitation and emission wavelengths of 443 and 484 nm, respectively.

Electron Microscopy. TEM was used to characterize the structural morphology and size of MSP2 fibrils both in the presence and in the absence of flavonoids. Protein samples (10 μL) were applied to 400 mesh copper grids coated with a thin layer of carbon for 2 min. Excess material was removed by blotting, and samples were negatively stained twice with 10 μL of a 2% (w/v)

uranyl acetate solution (Electron Microscopy Services). The grids were air-dried and viewed using a JEOL JEM-2010 transmission electron microscope operated at 80 kV.

NMR Spectroscopy. We prepared samples used for one-dimensional ^{1}H NMR by dissolving 1 mg of recombinant MSP2 in 500 μL of PBS containing 10% ^2H_2O and 0.05 μL of dioxane, which was added as an internal reference. We prepared the sample used for recording ^{1}H−^{15}N HSQC spectra by dissolving lyophilized, uniformly ^{15}N-labeled FC27 NT-MSP2 in PBS containing 10% ^2H_2O at a concentration of 2 mg/mL (87 μM). All samples were centrifuged at 13000 rpm for 10 min to remove any precipitate before being transferred to NMR tubes. NMR spectra were recorded at 5 °C on a Bruker DRX-600 spectrometer. ^{1}H chemical shifts were referenced with dioxane set at 3.751 ppm, and ^{15}N chemical shifts were referenced indirectly from ^{1}H using a γ_N:γ_H ratio of 0.101329118 (*27*). Two-dimensional ^{1}H−^{15}N HSQC spectra were recorded with 1024 (^{1}H) and 256 (^{15}N) points and spectral widths of 9 ppm (^{1}H) and 24 ppm (^{15}N). Unambiguous assignments were made for most of the cross-peaks in the ^{1}H−^{15}N HSQC spectrum of MSP2 based on published chemical shifts, making use of a pH titration to follow chemical shift changes from the acidic pH studied previously to the present conditions (*11*). For the EGCG titrations, a stock solution of EGCG (32 mM) was prepared in water, and aliquots from this stock were added to the ^{15}N-labeled FC27 NT-MSP2 NMR sample to give EGCG:MSP2 molar ratios of 1:1, 5:1, 10:1, and 20:1. One-dimensional ^{1}H and two-dimensional ^{1}H−^{15}N HSQC spectra were recorded after each EGCG addition. Similarly for baicalein and resveratrol titrations, stock solutions of 40 mM were prepared in [$^2H_6$]DMSO and aliquots from this stock were added to the ^{15}N-labeled FC27 NT-MSP2 NMR sample to give flavonoid:MSP2 molar ratios of 1:1, 5:1, 10:1, and 15:1. The final DMSO concentration in these samples was 1.5% (v/v). One-dimensional (1D) ^{1}H NMR spectra of the free flavonoids were also recorded under similar solution conditions. Spectra were processed using TOPSPIN (version 1.3, Bruker Biospin) and analyzed using XEASY (version 1.3.13).

Size-Exclusion Chromatography. Size-exclusion chromatography was performed using a Superdex 200 column on an AKTA FPLC system (GE Healthcare). FC27 NT-MSP2 (43 μM) was incubated with a 10-fold molar excess of EGCG and a 15-fold molar excess of baicalein and resveratrol or without the flavonoids for 1 week at 37 °C on a rotator. The samples were centrifuged at 13000 rpm for 10 min, and the supernatant was loaded onto a Superdex 200 column. Proteins were eluted in PBS buffer at a flow rate of 0.5 mL/min. The column was calibrated under similar conditions with thyroglobulin (670 kDa), bovine γ-globulin (156 kDa), ovalbumin (44 kDa), myoglobin (17 kDa), and vitamin B12 (1.35 kDa).

SDS−PAGE and Western Blotting. Monomeric MSP2, EGCG-treated MSP2, and fractions from SEC were analyzed by SDS−PAGE under reducing conditions on 12% Bis-Tris NuPAGE (Invitrogen) gels and silver stained. These samples were also analyzed by Western blotting using monoclonal antibodies (mAbs) 6D8 and 8G10 and rabbit antisera raised against FC27 MSP2-6H (*10*). Proteins (0.25 μg) were separated under reducing conditions on 4−12% Bis-Tris NuPAGE (Invitrogen) gels and then transferred to polyvinylidene difluoride (PVDF) membranes (Immobilon-P, Millipore) for Western blotting. The membranes were probed with purified mAbs [1 μg/mL in blotto (5% skim milk powder in PBS)] and rabbit antisera raised against FC27 MSP2-6H (1:1000 in blotto). After being washed, membranes were incubated (1 h) with the appropriate horseradish peroxidise-conjugated secondary antibody (Chemicon) (diluted 1:1000 in blotto). Binding was detected by enhanced chemiluminescence using the SuperSignal West Pico Chemiluminescent Substrate (Pierce).

EGCG Pull-Down Assay. EGCG was conjugated to CNBr-activated Sepharose 4B (GE Healthcare) as described previously (*28*). FC27 NT-MSP2 (20 μM) was incubated with 0.5 mL of EGCG-Sepharose 4B in PBS for 1 h at 4 °C. A synthetic peptide corresponding to the conserved N-terminal region of MSP2 (N-MSP2) was also bound to EGCG-Sepharose 4B. The beads were washed five times with PBS, and the proteins bound to the beads were analyzed by SDS−PAGE. Bovine serum albumin (BSA) (0.5 mg/mL) was allowed to bind to EGCG-Sepharose 4B as a negative control. FC27 NT-MSP2 was also allowed to bind to unconjugated Sepahrose 4B as a negative control.

Nitroblue Tetrazolium Staining. Nitroblue tetrazolium (NBT) (Sigma) staining was performed to detect protein-bound EGCG quinones (*29*). Proteins were separated by SDS−PAGE and electroblotted onto nitrocellulose membranes using an iBlot transfer kit (Invitrogen). The membrane was immersed in the glycinate/NBT solution [0.24 mM nitroblue tetrazolium in 2 M potassium glycinate (pH 10)] for 45 min in the dark. This resulted in a purple stain of quinone-bound protein bands. The membrane was washed and stored in 0.1 M sodium borate (pH 10).

Circular Dichroism Spectroscopy. Far-UV CD spectra were recorded on an Aviv 410SF CD spectrophotometer using a 1 mm path length cell. CD spectra were recorded with a step size of 0.5 nm, a bandwidth of 1 nm, and an averaging time of 2 s. Monomeric and polymeric protein samples were buffer exchanged into 10 mM phosphate buffer (pH 7.4) before CD measurements were performed. FC27 NT-MSP2 samples (10 μM) were incubated in the presence of varying amounts of EGCG (equimolar and 5-fold and 10-fold molar excesses) for 1 week at 37 °C on a rotator. Solutions containing corresponding amounts of EGCG alone were incubated in parallel. Similarly, FC27 NT-MSP2 samples (10 μM) were incubated in the presence of varying amounts of baicalein and resveratrol (equimolar and 5-fold and 15-fold molar excesses) for 1 week, and CD spectra were recorded. Baicalein and resveratrol stocks were prepared in methanol rather than DMSO, resulting in 1−0.5% methanol content in samples containing baicalein and resveratrol; the addition of methanol did not affect the kinetics of MSP2 fibril formation. CD spectra of the appropriate buffers and flavonoid solutions were recorded and subtracted from the corresponding protein spectra. All spectra were smoothed using a local smoothing function employing bisquare weighting and polynomial regression in Sigmaplot version 8.0 (SPSS Inc.).

RESULTS

Effect of Flavonoids on the Kinetics of Fibril Formation. The effects of the flavonoids on the kinetics of FC27 MSP2 fibril formation were analyzed using a ThT binding assay. In the absence of flavonoids, monomeric MSP2 formed amyloid-like fibrils by nucleation-dependent polymerization, characterized by a lag phase followed by an exponential increase in the level of fibril formation resulting in enhanced ThT fluorescence, as shown previously (*10*). In the presence of DMSO, MSP2 exhibited a marked increase in ThT fluorescence compared with the sample without DMSO (Figure 2). It is unclear whether this is due to the formation of more fibrils in the presence of DMSO or enhancement of ThT fluorescence by DMSO. When MSP2 was incubated with a 15-fold molar excess of resveratrol, there was a marked reduction in the maximum level of ThT fluorescence. Very low ThT fluorescence intensities

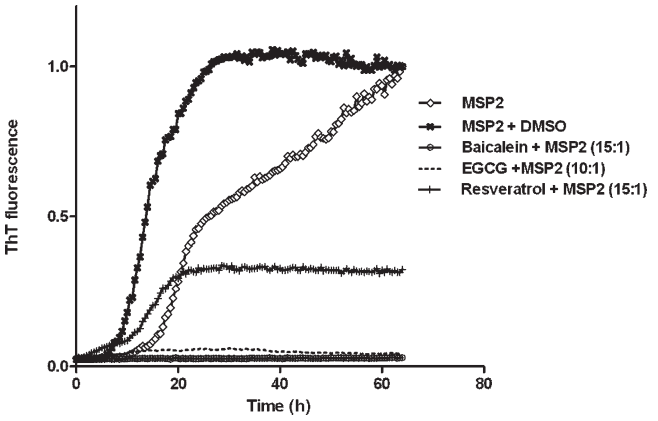

FIGURE 2: Effect of flavonoids on MSP2 fibrillogenesis as measured by ThT fluorescence. Kinetics of MSP2 fibril formation were measured in the presence of EGCG, baicalein, and resveratrol. FC27 MSP2-6H (40 μM) was incubated in the presence of a 10-fold molar excess of EGCG and a 15-fold molar excess each of baicalein and resveratrol, and ThT fluorescence was measured over a period of 64 h.

were seen when MSP2 was incubated in the presence of 10- and 15-fold molar excesses of EGCG and baicalein, respectively (Figure 2 and Figure S1 of the Supporting Information). Incubation of MSP2 with EGCG led to a dose-dependent decrease in ThT fluorescence (Figure S1), with inhibition of MSP2 fibrillation being evident even at stoichiometric concentrations of EGCG. MSP2 incubated with stoichiometric concentrations of baicalein displayed ThT fluorescence intensities similar to that of the MSP2 control in the presence of methanol (Figure S1), but a significant reduction in ThT fluorescence was observed when MSP2 was incubated with 5- and 15-fold molar excesses of baicalein (Figure S1). Dose-dependent inhibition of MSP2 fibrillogenesis was not evident for resveratrol (Figure S1).

TEM Analysis of MSP2 Fibril Formation. The effects of flavonoids on FC27 NT-MSP2 fibril formation and morphology were studied further by TEM. Negatively stained samples of recombinant FC27 NT-MSP2 contained long fibrils of varying lengths (Figure 3A). When FC27 NT-MSP2 was incubated with a 10-fold molar excess of EGCG, very few fibrils were formed; instead, numerous compact spherical oligomers were observed (Figure 3B). Incubation of FC27 NT-MSP2 with EGCG for 2 months did not result in further fibril formation that could be detected by EM (Figure 3C), which demonstrates the stability of these oligomers and suggests that the EGCG-stabilized oligomers are off-pathway aggregation products. Alternatively, EGCG may act by inhibiting the transition between this oligomeric state and the fibrillar state. Samples containing FC27 NT-MSP2 incubated with a 15-fold molar excess of baicalein or resveratrol also contained an abundance of long fibrils (Figure 3D,E). As the baicalein and resveratrol stock solutions were prepared in DMSO, a sample of MSP2 incubated with DMSO was also examined by TEM and found to contain numerous fibrils (Figure 3F). These observations are in contrast to the results of the ThT binding assay, which showed basal levels of ThT fluorescence intensity when MSP2 was incubated with baicalein (Figure 2 and Figure S1), and suggest that baicalein may interfere with ThT fluorescence by displacing ThT bound to MSP2 and reducing its fluorescence yield rather than by inhibiting fibril formation (*30*).

NMR Studies of Interactions of Flavonoids with MSP2. One-dimensional NMR spectra of FC27 NT-MSP2 under physiological conditions (PBS, pH 7.2) displayed limited chemical shift dispersion and considerable peak overlap, consistent with previous results showing that MSP2 is intrinsically unstructured (*10*, *11*). One−dimensional ^{1}H and two−dimensional ^{1}H−^{15}N HSQC spectra of FC27 NT-MSP2 were recorded in the presence of different molar ratios (equimolar and 5-, 10-, 15-, and 20-fold molar excesses) of EGCG, baicalein, and resveratrol. One−dimensional spectra of the free flavonoids were also recorded under similar solution conditions (Figure S2 of the Supporting Information).

Resonances of MSP2 and EGCG alone were sharp (Figure S3 of the Supporting Information), whereas titration of MSP2 with EGCG led to significant broadening of EGCG resonances, particularly those at 5.5, 6.1, and 6.5 ppm (Figure 4A). Some of the MSP2 resonances also exhibited broadening in a dose-dependent fashion (Figure 4B and Figure S3). In addition, EGCG induced concentration-dependent upfield changes in chemical shift for a number of MSP2 resonances (Figure S4 of the Supporting Information). These changes in chemical shift are indicative of a relatively weak interaction between EGCG and MSP2, in fast exchange on the chemical shift time scale. The resonances most perturbed by EGCG were those corresponding to the conserved N- and C-terminal regions, with the variable central region less affected. At an EGCG:MSP2 ratio of 20:1, significant uniform loss of signal intensity was observed, and the sample suffered a further loss of peak intensity on incubation for 1 week (Figure 4B). As demonstrated above, this is likely due to formation of MSP2 oligomers, the spectrum of which would be too broad to be observed.

Titration of MSP2 with baicalein led to broadening of the baicalein resonances at 6.71 and 6.53 ppm (Figure 4C), but no significant changes in chemical shift or line width for MSP2 resonances, even at a 15-fold molar excess of baicalein (Figure S5 of the Supporting Informartion). However, upon incubation of baicalein with MSP2 (15:1 baicalein:MSP2 ratio) for 1 week, several resonances in the conserved N-terminal region of MSP2 displayed line broadening and subsequently disappeared (Figure 4D). Residues that exhibited significant line broadening on incubation were exclusively from the conserved N-terminal region, residues 1−25. Resonances from the rest of the molecule did not show any significant change in line width and remained visible even after incubation for 1 month. However, upon storage for 1 month, the samples showed a ~50% reduction in overall peak intensity, indicating some aggregation of MSP2.

In contrast to EGCG and baicalein, titration of MSP2 with resveratrol (Figure S6 of the Supporting Informartion) led to no significant change in chemical shift or line width, even after incubation for 1 week (Figure 4E,F). However, an attenuation of resveratrol resonances was observed, which could be due to oxidative aggregation of the compound upon incubation (Figure 4E).

Characterization of Flavonoid-Stabilized MSP2 Oligomers. To gain further insight into the oligomeric state of MSP2 stabilized in the presence of flavonoids, size-exclusion chromatography was performed. Untreated MSP2 eluted from the size-exclusion column as a single peak with an apparent molecular mass of ~100 kDa (Figure 5A), which is larger than the expected mass (23 kDa) because of the intrinsically unstructured nature of MSP2 (*10*). When incubated with EGCG, MSP2 eluted from the Superdex 200 column as a series of oligomers; this was confirmed by SDS−PAGE analysis, which showed that MSP2 had formed an oligomeric series (Figure 5B,C). The stability of these oligomers in SDS−PAGE sample buffer suggests that they are stabilized by covalent bonds.

In contrast to the EGCG-treated sample, there was no evidence of soluble oligomers in the baicalein- and resveratrol-treated MSP2 samples. These samples contained a large proportion of

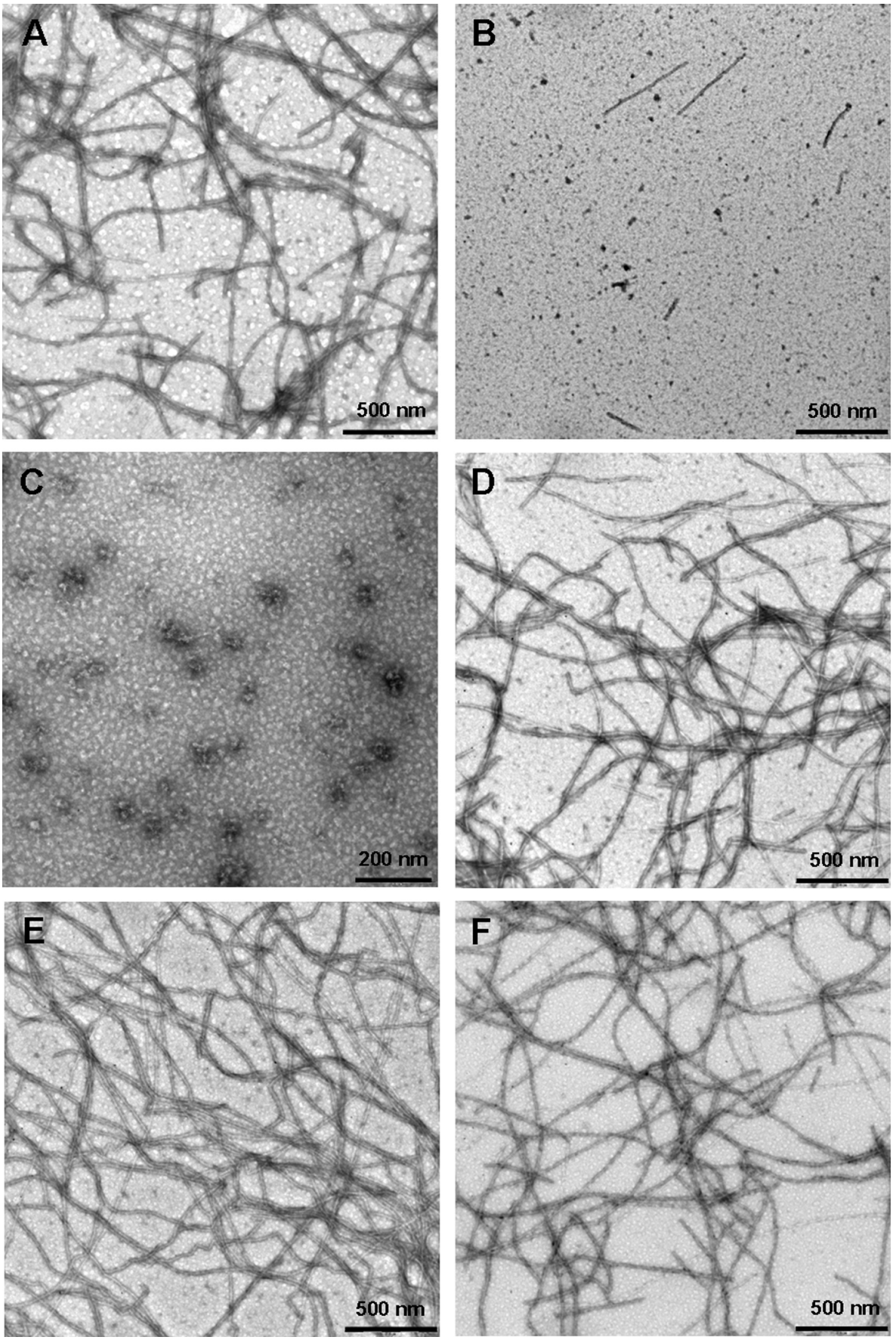

FIGURE 3: Analysis of negatively stained MSP2 by TEM. TEM images of FC27 NT-MSP2 after incubation for 3 days (A) in PBS and (B) in the presence of a 10-fold molar excess of EGCG. (C) FC27 NT-MSP2 incubated with EGCG for 2 months. FC27 NT-MSP2 after incubation for 3 days in the presence of (D) a 15-fold molar excess of baicalein and (E) resveratrol or (F) 1.5% (v/v) DMSO.

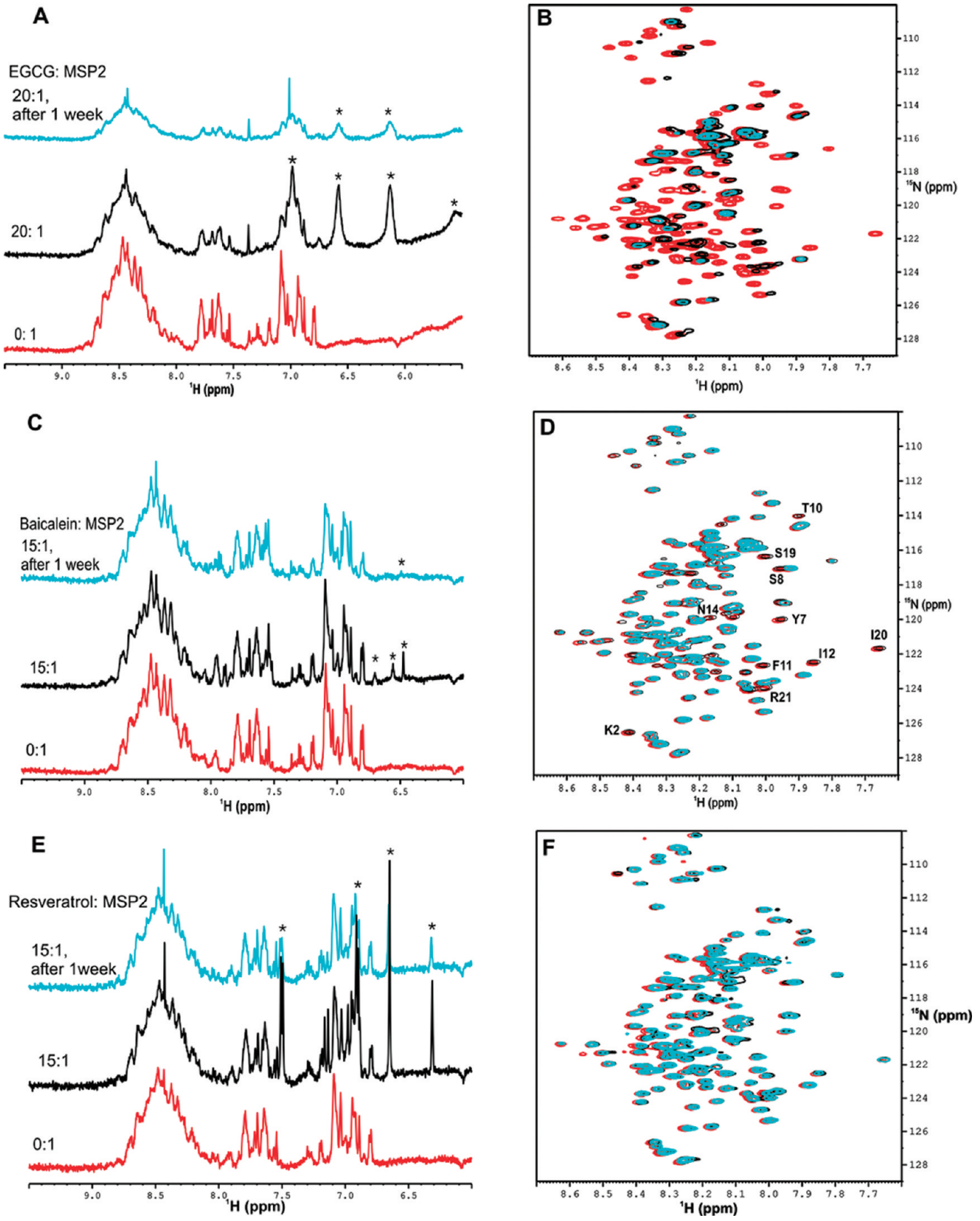

FIGURE 4: NMR spectra of flavonoid binding to MSP2. (A) Amide and aromatic region of the ^{1}H 1D spectra of FC27 NT-MSP2 titrated with EGCG. EGCG resonances are labeled with asterisks. (B) Superposition of ^{1}H−^{15}N HSQC spectra of FC27 NT-MSP2 in the absence (red) and in the presence of EGCG (20:1 EGCG:MSP2) before (black) and after incubation for 1 week (cyan). (C) Amide and aromatic region of the ^{1}H 1D spectra of FC27 NT-MSP2 titrated with baicalein. Baicalein resonances are labeled with asterisks. (D) Superposition of ^{1}H−^{15}N HSQC spectra of FC27 NT-MSP2 in the absence (red) and presence of baicalein (15:1 baicalein:MSP2) before (black) and after incubation for 1 week (cyan). (E) Amide and aromatic region of the ^{1}H 1D spectra of FC27 NT-MSP2 titrated with resveratrol. Resveratrol resonances are labeled with asterisks. (F) Superposition of ^{1}H−^{15}N HSQC spectra of FC27 NT-MSP2 in the absence (red) and presence of resveratrol (15:1 resveratrol:MSP2) before (black) and after incubation for 1 week (cyan). The spectra were recorded in PBS at 5 °C and 600 MHz.

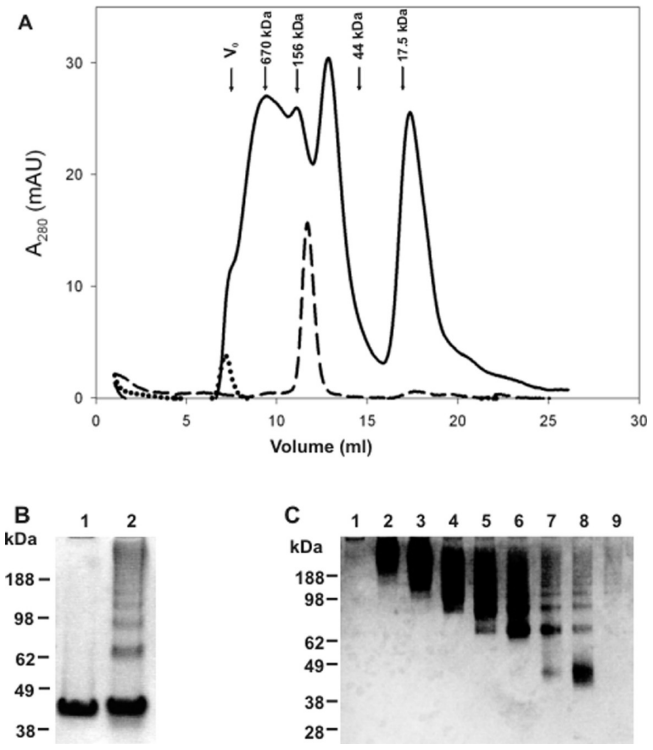

FIGURE 5: EGCG stabilizes soluble oligomeric species of MSP2. (A) Size-exclusion chromatography of MSP2 monomer (– – –), MSP2 fibrils (· · ·), and EGCG-stabilized oligomers (—). (B) SDS–PAGE of EGCG-treated MSP2. Lanes 1 and 2 contained monomeric MSP2 and EGCG-treated MSP2, respectively. FC27 NT-MSP2 (43 μM) was incubated with a 10-fold molar excess of EGCG for 1 week. (C) SDS–PAGE analysis of SEC-purified fractions of EGCG-stabilized oligomers. Lanes 1–9 contained fractions eluted from the Superdex 200 column at 7, 8, 9, 10, 11, 12, 13, 14, and 18 mL, respectively.

high-molecular weight aggregates eluting in the void volume (Figure S7 of the Supporting Information), consistent with EM results, which showed the presence of significant amounts of fibrillar material in these samples.

We also tested whether EGCG-stabilized MSP2 oligomers were recognized by antibodies produced against recombinant FC27 MSP2-6H. The mAbs used in these analyses were 6D8 and 8G10, which recognize epitopes in the conserved N-terminal region and the central variable region of MSP2, respectively (*10*), and a rabbit antiserum raised against MSP2. EGCG-stabilized oligomers reacted with all antibodies, indicating that these epitopes are available following EGCG binding (Figure 6).

EGCG Binds MSP2. A recent study has shown that EGCG binds preferentially to unfolded proteins (*17*). To further confirm that EGCG can bind directly to MSP2, we used an in vitro EGCG pull-down assay (*28*, *31*). FC27 NT-MSP2 bound to EGCG-Sepharose 4B beads (Figure 7A), whereas the folded control protein, BSA, did not bind to these beads and eluted in the flow-through (Figure 7D). In contrast, FC27 NT-MSP2 did not bind to unconjugated Sepharose 4B beads (Figure 7B). Our NMR data suggested that EGCG interacted with the N-terminus of MSP2. This interaction was confirmed using a synthetic peptide (N-MSP2) corresponding to the first 25 residues of MSP2 in an EGCG pull-down assay (Figure 7C, lane 1).

Detection of MSP2-Bound EGCG Quinones. An NBT staining assay, which detects protein-bound quinones (*17*, *29*, *32*), was used to further characterize the binding of EGCG to MSP2. Samples of freshly prepared monomeric FC27 NT-MSP2 were incubated in the absence of EGCG and the presence of equimolar EGCG and 5- and 10-fold excesses of EGCG for 1 week. These samples were separated by SDS–PAGE, electroblotted onto a nitrocellulose membrane, and stained with NBT. NBT stained the MSP2 oligomers, but not the monomer (Figure 8B). Similarly, no color reaction occurred when EGCG was absent or incubated with monomeric MSP2 for 10 min (Figure S8 of the Supporting Information). These results indicate that MSP2 is covalently cross-linked by EGCG-derived quinones to form oligomers. An increase in NBT stain intensity was observed for the MSP2 oligomeric bands in the 10:1 and 5:1 EGCG/MSP2 samples compared to the 1:1 sample, indicating that the formation of EGCG cross-linked MSP2 oligomers is dose-dependent (Figure 8B). The formation of MSP2–EGCG quinone complexes was related to the aging of EGCG and the subsequent autoxidation to form quinones.

Effect of Flavonoids on the Secondary Structure of MSP2. Monomeric FC27 NT-MSP2 has a CD spectrum indicative of a protein that is largely random coil, with an ellipticity minimum between 200 and 210 nm (Figure 9). Previous studies have shown that conformational changes associated with the polymerization of MSP2 result in an increased β-sheet content (*10*). Far-UV CD spectra of FC27 NT-MSP2 were acquired in the presence of different molar ratios of EGCG to study the effect of EGCG binding on the secondary structure of MSP2. In EGCG-treated samples, MSP2 maintained its unstructured conformation (Figure 9). This is consistent with the relatively small magnitude and uniform sign of the chemical shift changes observed on titration of MSP2 with EGCG and suggests that EGCG blocks fibrillogenesis by preventing the conformational transition of MSP2 from a random coil to amyloidogenic β-sheet structure. In contrast, FC27 NT-MSP2 incubated in the presence of baicalein and resveratrol exhibited CD spectra characteristic of a β-sheet rich structure similar to that of the control sample incubated in PBS (Figure S9 of the Supporting Information), indicating that these flavonoids did not prevent the conformational transition of MSP2 from a random coil to a β-sheet-like structure and, therefore, were unable to inhibit MSP2 fibrillogenesis.

DISCUSSION

MSP2, one of the most abundant proteins on the *P. falciparum* merozoite surface, is intrinsically unstructured and prone to form amyloid-like fibrils under physiological conditions (*10*). The propensity of MSP2 to form fibrils in solution, the unstable nature of these fibrils, and the various pathologies associated with amyloid fibrils are issues that may have an impact on vaccine development programs with this antigen. Finding small molecule inhibitors that specifically inhibit fibril formation is therefore potentially valuable in the development of MSP2 as a vaccine candidate.

In this study, we have investigated the effects of the flavonoids EGCG, baicalein, and resveratrol on the amyloid fibril assembly pathway of MSP2. Data from ThT binding assays and TEM, NMR, and CD studies suggest that EGCG inhibits the formation of fibrils by MSP2. In contrast, although ThT binding assays suggest inhibition of MSP2 fibrillogenesis by baicalein and resveratrol, TEM and CD studies of baicalein- and resveratrol-treated MSP2 samples revealed the presence of significant quantities of fibrils. These results clearly show that baicalein and resveratrol interfere with the ThT fluorescence assay. A recent study has shown that resveratrol can significantly bias the ThT fluorescence assay by competitively binding with ThT for the fibrils (*30*). Our data suggest that the ThT binding assays can lead to false positives in

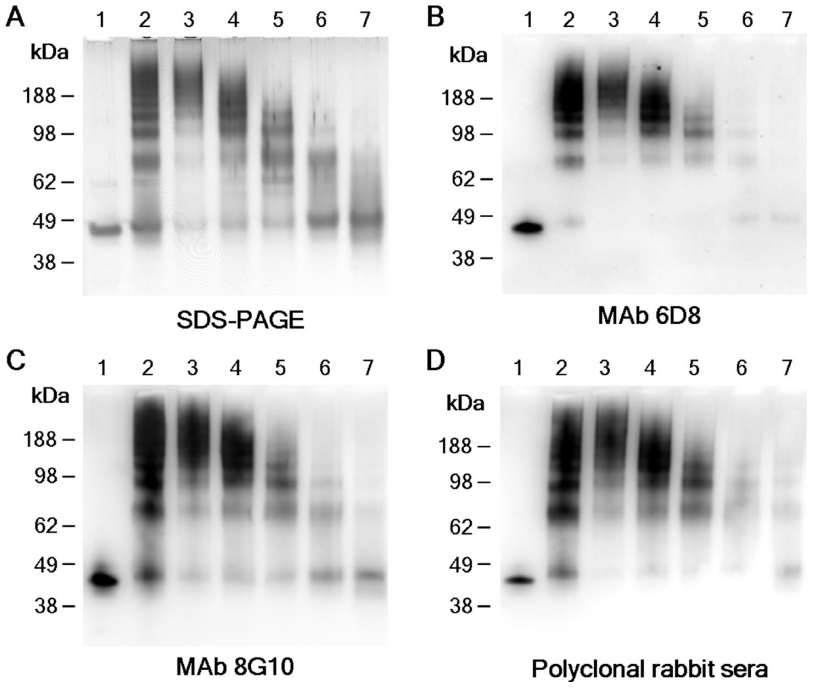

FIGURE 6: Analysis of EGCG-stabilized MSP2 oligomers following SEC. Proteins eluted from the Superdex 200 column were analyzed on a (A) silver-stained SDS−PAGE gel and by Western blotting experiments probed with (B) mAb 6D8, (C) mAb 8G10, and (D) rabbit sera raised against FC27 MSP2-6H. Lanes contained FC27 NT-MSP2 (lane 1), EGCG-treated FC27 NT-MSP2 (lane 2), and SEC-purified fractions of EGCG-stabilized MSP2 oligomers (lanes 3−7).

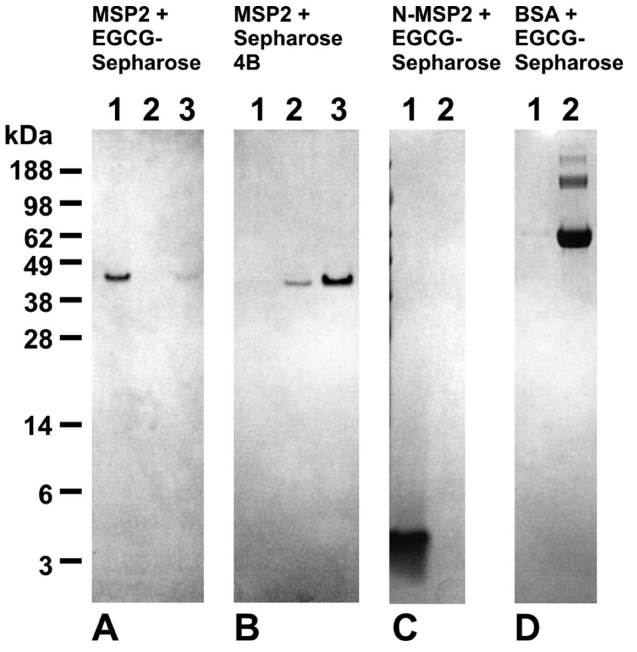

FIGURE 7: EGCG pull-down assay. (A) FC27 NT-MSP2, (C) N-MSP2, and (D) BSA were incubated with EGCG-Sepharose 4B resin. After being washed, the proteins bound to the resin were analyzed by SDS−PAGE. (B) FC27 NT-MSP2 was bound to unconjugated Sepharose 4B as a negative control. Lanes 1−3 contained protein eluted from Sepharose beads, column wash, and flow-through, respectively, in panels A and B. Lanes 1 and 2 contained protein eluted from Sepharose beads and flow-through, respectively, in panels C and D.

screens for inhibitors of fibrillogenesis, and it is therefore important to confirm the inhibitory potential of such molecules using additional biochemical and biophysical techniques.

TEM, SEC, and SDS−PAGE analyses showed that highly stable oligomers were formed in EGCG-treated samples of MSP2. This suggests that the EGCG binds to MSP2, suppressing the assembly of fibrils and redirecting the pathway into unstructured, soluble oligomers. The mechanism by which this occurs has yet to be determined. Our NMR data indicate that inhibition of MSP2 fibril formation by EGCG involves initial, presumably noncovalent, interactions of EGCG with monomeric MSP2, followed by EGCG-mediated MSP2 oligomerization. During EGCG-mediated MSP2 oligomerization, most of the resonances from the conserved N-terminal residues, as well as some from the conserved C-terminal region, undergo line broadening and disappear, while many of the resonances from the central variable region remain visible, albeit with reduced intensity, even after incubation for 1 week (Figure 4B). Similarly, specific broadening was observed for several resonances in the conserved N-terminal region of MSP2 upon incubation with baicalein (Figure 4D). This suggests that the conserved N-terminal region of MSP2, which forms the proteinase K-resistant core of fibrils formed by MSP2 (*12*, *13*), plays a role in flavonoid-mediated oligomerization of MSP2, whereas the central variable region maintains significant flexibility in the oligomeric species. Consistent with this, CD spectra of the EGCG-stabilized MSP2 oligomers show that the natively unfolded conformation of MSP2 is preserved during EGCG-mediated oligomerization (Figure 9). Thus, our data are consistent with recent studies showing that the inhibition of fibril formation by flavonoids is a complex process involving several successive steps, including noncovalent binding of the flavonoid to the protein, followed by covalent modification of the protein by the flavonoid (*33*). It has been reported that there is a strong correlation between the autoxidation potential of flavonoids and their inhibitory activity, this oxidation potential being determined by the presence of vicinal hydroxyl groups and their ability to form quinones (*33*). Comparison of the structures of the three flavonoids investigated here reveals an association between the oxidation potential and their inhibitory activity. EGCG has several vicinal hydroxyl groups and hence a higher oxidation potential than resveratrol, which lacks vicinal hydroxyl groups

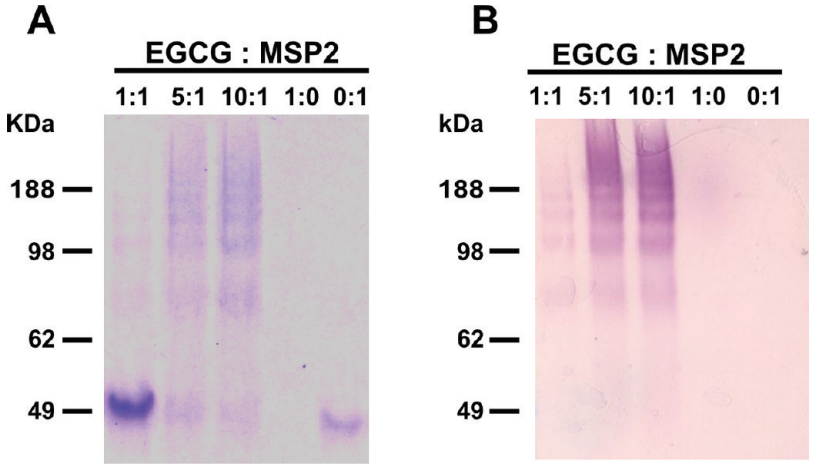

FIGURE 8: Covalent modification of MSP2 by EGCG quinones. Comparison of (A) a Coomassie-stained SDS−PAGE gel and (B) a nitroblue tetrazolium-stained nitrocellulose membrane of MSP2 samples. FC27 NT-MSP2 was incubated for 1 week in the presence (molar ratios of EGCG to MSP2 are indicated above the gel) and absence of EGCG.

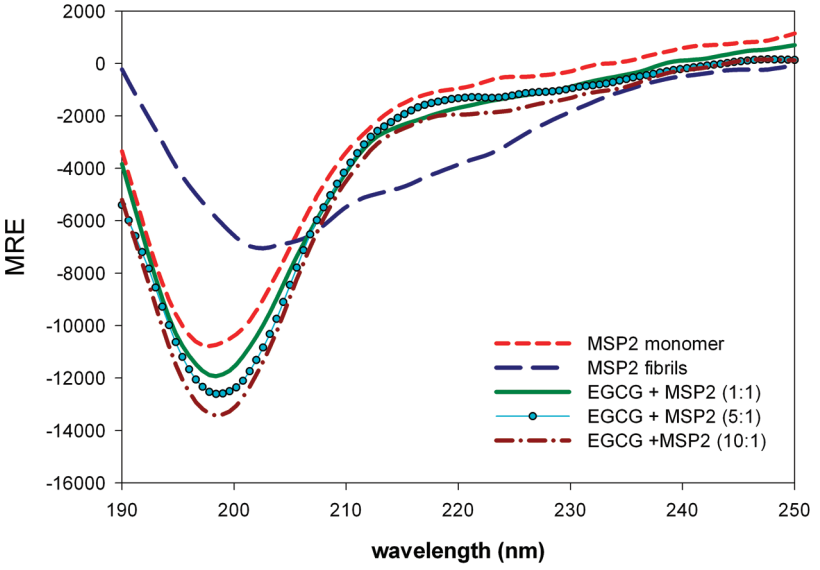

FIGURE 9: EGCG inhibits β-sheet formation in MSP2. Far-UV CD spectra of FC27 NT-MSP2 were recorded in the absence and presence of equimolar EGCG as well as 5- and 10-fold excesses. All samples were incubated for 1 week.

(Figure 1). We have shown in this study that EGCG forms quinones that bind to MSP2 (Figure 8). Preliminary mass spectrometry data suggest that covalent modification of MSP2 by EGCG and baicalein occurs (data not shown). It is possible that EGCG−quinone adducts cross-link the MSP2 monomers to form stable oligomeric complexes. Interestingly, binding of EGCG quinones to MSP2 does not seem to affect the other structural properties of MSP2 (Figure 9), and the modified MSP2 retained reactivity with a range of antibodies (Figure 6). Recent studies on α-synuclein have shown that the amino groups on the lysine side chains undergo nucleophilic attack by the quinones to form Schiff bases (*18*, *33*, *34*). The side chains of lysine residues in MSP2 are the probable reactive sites for covalent modification by EGCG-bound quinones, but there is no evidence from our NMR data to support this. The exact mechanism by which EGCG stabilizes the MSP2 oligomers and prevents fibril formation is still not clear, and further studies will be necessary to elucidate the mechanism.

The intrinsically unstructured nature of MSP2 has been suggested as a possible cause of the reduced efficiency of the anti-MSP2 antibody response, as well as the poor efficacy of these antibodies in blocking merozoite invasion in vitro (*10*). The antibody response to MSP2 may be characterized by specificities to many of the alternative conformations sampled by the molecule in solution, which may not include the dominant and more restrained conformation adopted by MSP2 on the merozoite surface (*10*, *11*). There is direct evidence that MSP2 forms homo-oligomers on the merozoite surface, and this might be an effective strategy for including a recombinant homopolymer of MSP2 in a vaccine (*10*). Small molecules like EGCG can change the equilibrium between various protein conformations in solution and stabilize oligomeric forms of the protein. In this study, we have shown that EGCG stabilizes oligomeric forms of MSP2 that neither disassemble under denaturing conditions nor assemble into fibrils upon incubation. It will be of interest to examine in detail the immunogenicity of the EGCG-stabilized MSP2 oligomers, but the covalent modification of MSP2 by EGCG would most likely not be acceptable in a human vaccine formulation.

ACKNOWLEDGMENT

We thank Drs. Michael Foley, Jeff Babon, and Andrew Low for helpful discussions. We thank Dr. Matthew Perugini and

members of his lab at the Bio21 Institute (University of Melbourne, Melbourne, Australia) for access to their CD spectrometer.

SUPPORTING INFORMATION AVAILABLE

Figures illustrating the kinetics of fibril formation by MSP2 and dose-dependent inhibition by flavonoids, NMR spectra of MSP2 titrated with flavonoids, NBT staining of MSP2 in the presence of EGCG, and SEC profiles and CD spectra of MSP2 in the presence of baicalein and resveratrol. This material is available free of charge via the Internet at http://pubs.acs.org.

REFERENCES

1. Snow, R. W., Guerra, C. A., Noor, A. M., Myint, H. Y., and Hay, S. I. (2005) The global distribution of clinical episodes of *Plasmodium falciparum* malaria. *Nature 434*, 214–217.
2. World Health Organization (2009) World Malaria Report 2009, World Health Organization Press, Geneva.
3. Sachs, J., and Malaney, P. (2002) The economic and social burden of malaria. *Nature 415*, 680–685.
4. Smythe, J. A., Coppel, R. L., Brown, G. V., Ramasamy, R., Kemp, D. J., and Anders, R. F. (1988) Identification of two integral membrane proteins of *Plasmodium falciparum*. *Proc. Natl. Acad. Sci. U.S.A. 85*, 5195–5199.
5. Gerold, P., Schofield, L., Blackman, M. J., Holder, A. A., and Schwarz, R. T. (1996) Structural analysis of the glycosyl-phosphatidylinositol membrane anchor of the merozoite surface proteins-1 and -2 of *Plasmodium falciparum*. *Mol. Biochem. Parasitol. 75*, 131–143.
6. Genton, B., Betuela, I., Felger, I., Al-Yaman, F., Anders, R. F., Saul, A., Rare, L., Baisor, M., Lorry, K., Brown, G. V., Pye, D., Irving, D. O., Smith, T. A., Beck, H. P., and Alpers, M. P. (2002) A recombinant blood-stage malaria vaccine reduces *Plasmodium falciparum* density and exerts selective pressure on parasite populations in a phase 1-2b trial in Papua New Guinea. *J. Infect. Dis. 185*, 820–827.
7. Smythe, J. A., Coppel, R. L., Day, K. P., Martin, R. K., Oduola, A. M., Kemp, D. J., and Anders, R. F. (1991) Structural diversity in the *Plasmodium falciparum* merozoite surface antigen 2. *Proc. Natl. Acad. Sci. U.S.A. 88*, 1751–1755.
8. Fenton, B., Clark, J. T., Khan, C. M., Robinson, J. V., Walliker, D., Ridley, R., Scaife, J. G., and McBride, J. S. (1991) Structural and antigenic polymorphism of the 35- to 48-kilodalton merozoite surface antigen (MSA-2) of the malaria parasite *Plasmodium falciparum*. *Mol. Cell. Biol. 11*, 963–971.
9. Thomas, A. W., Carr, D. A., Carter, J. M., and Lyon, J. A. (1990) Sequence comparison of allelic forms of the *Plasmodium falciparum* merozoite surface antigen MSA2. *Mol. Biochem. Parasitol. 43*, 211–220.
10. Adda, C. G., Murphy, V. J., Sunde, M., Waddington, L. J., Schloegel, J., Talbo, G. H., Vingas, K., Kienzle, V., Masciantonio, R., Howlett, G. J., Hodder, A. N., Foley, M., and Anders, R. F. (2009) *Plasmodium falciparum* merozoite surface protein 2 is unstructured and forms amyloid-like fibrils. *Mol. Biochem. Parasitol. 166*, 159–171.
11. Zhang, X., Perugini, M. A., Yao, S., Adda, C. G., Murphy, V. J., Low, A., Anders, R. F., and Norton, R. S. (2008) Solution conformation, backbone dynamics and lipid interactions of the intrinsically unstructured malaria surface protein MSP2. *J. Mol. Biol. 379*, 105–121.
12. Low, A., Chandrashekaran, I. R., Adda, C. G., Yao, S., Sabo, J. K., Zhang, X., Soetopo, A., Anders, R. F., and Norton, R. S. (2007) Merozoite surface protein 2 of *Plasmodium falciparum*: Expression, structure, dynamics, and fibril formation of the conserved N-terminal domain. *Biopolymers 87*, 12–22.
13. Yang, X., Adda, C. G., Keizer, D. W., Murphy, V. J., Rizkalla, M. M., Perugini, M. A., Jackson, D. C., Anders, R. F., and Norton, R. S. (2007) A partially structured region of a largely unstructured protein, *Plasmodium falciparum* merozoite surface protein 2 (MSP2), forms amyloid-like fibrils. *J. Pept. Sci. 13*, 839–848.
14. Porat, Y., Abramowitz, A., and Gazit, E. (2006) Inhibition of amyloid fibril formation by polyphenols: Structural similarity and aromatic interactions as a common inhibition mechanism. *Chem. Biol. Drug Des. 67*, 27–37.
15. Crozier, A., Jaganath, I. B., and Clifford, M. N. (2009) Dietary phenolics: Chemistry, bioavailability and effects on health. *Nat. Prod. Rep. 26*, 1001–1043.
16. Li-Weber, M. (2009) New therapeutic aspects of flavones: The anticancer properties of *Scutellaria* and its main active constituents Wogonin, Baicalein and Baicalin. *Cancer Treat. Rev. 35*, 57–68.
17. Ehrnhoefer, D. E., Bieschke, J., Boeddrich, A., Herbst, M., Masino, L., Lurz, R., Engemann, S., Pastore, A., and Wanker, E. E. (2008) EGCG redirects amyloidogenic polypeptides into unstructured, off-pathway oligomers. *Nat. Struct. Mol. Biol. 15*, 558–566.
18. Zhu, M., Rajamani, S., Kaylor, J., Han, S., Zhou, F., and Fink, A. L. (2004) The flavonoid baicalein inhibits fibrillation of α-synuclein and disaggregates existing fibrils. *J. Biol. Chem. 279*, 26846–26857.
19. Hong, D. P., Fink, A. L., and Uversky, V. N. (2008) Structural characteristics of α-synuclein oligomers stabilized by the flavonoid baicalein. *J. Mol. Biol. 383*, 214–223.
20. Hudson, S. A., Ecroyd, H., Dehle, F. C., Musgrave, I. F., and Carver, J. A. (2009) (−)-Epigallocatechin-3-gallate (EGCG) maintains κ-casein in its pre-fibrillar state without redirecting its aggregation pathway. *J. Mol. Biol. 392*, 689–700.
21. Mandel, S. A., Amit, T., Weinreb, O., Reznichenko, L., and Youdim, M. B. (2008) Simultaneous manipulation of multiple brain targets by green tea catechins: A potential neuroprotective strategy for Alzheimer and Parkinson diseases. *CNS Neurosci. Ther. 14*, 352–365.
22. Ehrnhoefer, D. E., Duennwald, M., Markovic, P., Wacker, J. L., Engemann, S., Roark, M., Legleiter, J., Marsh, J. L., Thompson, L. M., Lindquist, S., Muchowski, P. J., and Wanker, E. E. (2006) Green tea (−)-epigallocatechin-gallate modulates early events in huntingtin misfolding and reduces toxicity in Huntington's disease models. *Hum. Mol. Genet. 15*, 2743–2751.
23. Jang, J. H., and Surh, Y. J. (2003) Protective effect of resveratrol on β-amyloid-induced oxidative PC12 cell death. *Free Radical Biol. Med. 34*, 1100–1110.
24. Radovan, D., Opitz, N., and Winter, R. (2009) Fluorescence microscopy studies on islet amyloid polypeptide fibrillation at heterogeneous and cellular membrane interfaces and its inhibition by resveratrol. *FEBS Lett. 583*, 1439–1445.
25. Mishra, R., Sellin, D., Radovan, D., Gohlke, A., and Winter, R. (2009) Inhibiting islet amyloid polypeptide fibril formation by the red wine compound resveratrol. *ChemBioChem 10*, 445–449.
26. LeVine, H., III (1999) Quantification of β-sheet amyloid fibril structures with Thioflavin T. *Methods Enzymol. 309*, 274–284.
27. Wishart, D. S., Bigam, C. G., Yao, J., Abildgaard, F., Dyson, H. J., Oldfield, E., Markley, J. L., and Sykes, B. D. (1995) ^{1}H, ^{13}C and ^{15}N chemical shift referencing in biomolecular NMR. *J. Biomol. NMR 6*, 135–140.
28. Ermakova, S., Choi, B. Y., Choi, H. S., Kang, B. S., Bode, A. M., and Dong, Z. (2005) The intermediate filament protein vimentin is a new target for epigallocatechin gallate. *J. Biol. Chem. 280*, 16882–16890.
29. Paz, M. A., Fluckiger, R., Boak, A., Kagan, H. M., and Gallop, P. M. (1991) Specific detection of quinoproteins by redox-cycling staining. *J. Biol. Chem. 266*, 689–692.
30. Hudson, S. A., Ecroyd, H., Kee, T. W., and Carver, J. A. (2009) The Thioflavin T fluorescence assay for amyloid fibril detection can be baised by the presence of exogenous compounds. *FEBS J. 276*, 5960–5972.
31. He, Z., Tang, F., Ermakova, S., Li, M., Zhao, Q., Cho, Y. Y., Ma, W. Y., Choi, H. S., Bode, A. M., Yang, C. S., and Dong, Z. (2008) Fyn is a novel target of (−)-epigallocatechin gallate in the inhibition of JB6 Cl41 cell transformation. *Mol. Carcinog. 47*, 172–183.
32. Zhou, W., Gallagher, A., Hong, D. P., Long, C., Fink, A. L., and Uversky, V. N. (2009) At low concentrations, 3,4-dihydroxyphenylacetic acid (DOPAC) binds non-covalently to α-synuclein and prevents its fibrillation. *J. Mol. Biol. 388*, 597–610.
33. Meng, X., Munishkina, L. A., Fink, A. L., and Uversky, V. N. (2009) Molecular mechanisms underlying the flavonoid-induced inhibition of α-synuclein fibrillation. *Biochemistry 48*, 8206–8224.
34. Li, H. T., Lin, D. H., Luo, X. Y., Zhang, F., Ji, L. N., Du, H. N., Song, G. Q., Hu, J., Zhou, J. W., and Hu, H. Y. (2005) Inhibition of α-synuclein fibrillization by dopamine analogs via reaction with the amino groups of α-synuclein. Implication for dopaminergic neurodegeneration. *FEBS J. 272*, 3661–3672.